[January, 1983] © *1983 The Chemical Society of Japan* *Bull. Chem. Soc. Jpn.*, ***56***, *1—5 (1983)* 1

The Polarization Characteristics and the Thickness of the Catalyst Layers in Fuel Cell Electrodes

Tadao KENJO* and Noriyuki NAKAJIMA†
Department of Applied Science for Energy, Faculty of Engineering, Muroran Institute of Technology, Mizumoto-cho, Muroran 050

(Received January 14, 1982)

The polarization characteristics of poly(tetrafluoroethylene)-bonded Raney nickel hydrogen- and silver oxygen-electrodes have been measured as a function of the thickness of the catalyst layer, and the polarization curves of these electrodes have been analyzed on the basis of the electrolyte film model. The observed polarization curves were divided into several segments and a linear polarization-current equation, derived from the model, has been applied to each segment. The performance of the electrodes approaches asymptotically to an upper limit with the thickening of the catalyst layers. The profiles of the faradayic current density across the electrode wall have been estimated for both electrodes. In contrast with the almost flat profiles of the Raney nickel electrodes, the current densities for the silver electrodes are localized on the liquid side of the electrodes; a thin area of the catalyst layer ranging from the electrode-face/electrolyte interface to 5.3×10^{-3} cm distance sustains most of the load current at a polarization of 220 mV. The catalytic activities of both the silver and Raney nickel catalysts are enhanced with progression of the polarization while the resistivities of the electrolyte film maintained essentially constant. A slight surface oxidation for the Raney nickel and a surface reduction for the silver catalysts have been suggested as probable explanations for the enhanced catalytic activities observed.

The performance of Raney nickel hydrogen-electrodes is markedly improved with increasing catalyst loading[1,2] while that of silver oxygen-electrodes is not so sensitive to the change of the loading as the hydrogen-electrodes.[3,4] The present study involves an attempt to explain this difference on the basis of the electrolyte film model.

The feature of this model is the thin electrolyte film covering the catalyst surface.[1,5,6] Owing to the ionic conductivity of the film the electrode reaction takes place not only on the electrode-face/electrolyte interface but also on the portion of the catalyst located at a distance from the interface. The load current is sustained by the electrode reaction occurring in this zonal area so that the performance of the electrode depends upon the thickness of the catalyst layer as well as on the geometrical working area of the electrode. If the reaction zone extends toward the gas side in a long range, a good performance can be expected when a thick electrode is used. If it is short range, a thin electrode suffices to yield the performance of the upper limit for the catalyst used.

The polarization characteristics and the thickness of the reaction zone are determined by the catalytic activity and the film resistivity. Mund and his coworkers have calculated these parameter values from the polarization data, assuming a linear polarization-faradayic current relation.[1,5] The formula derived from this assumption however cannot be applied to curved polarization characteristics as is observed in the present study. The more rigorous formula that is applicable to curves, is derived from the assumption that the faradayic current is an exponential function of the polarization, but complicated mathematical calculations are required for the derivation of the potential-current relation.[7,8] In the present study, to apply a linear function to curves, the polarization curves observed are divided into several segments that can be regarded as straight lines, and a linear potential-current relation is applied to each segment.

This analytical method for the polarization data is applied to the foregoing hydrogen and oxygen electrodes to estimate the catalytic activities and the film resistivities. These parameter values should explain why the Raney nickel electrodes differ from the silver electrodes in the performance-catalyst loading relationship. Setting desired parameter values that are not yet realized in the experiment, one can calculate polarization curves for unreal electrodes. This may provide us with some hints and orientations for improving the electrode performance.

Experimental

Preparation of the Raney Nickel Catalyst. An ingot containing 40% Ni (99.95% purity) and 60% Al (99.99% purity) was prepared by using an induction furnace. The ingot obtained was crushed and powdered to a particle size of less than 37 μm. The aluminium was leached with a 6 M KOH solution (1 M=1 mol $\mathrm{dm^{-3}}$) at 80 °C for 5 h. The Raney nickel thus obtained was washed with water and methyl alcohol.

Preparation of the Silver Catalyst. Ten grams of silver nitrate (guaranteed reagent, Yoneyama Chemical Co., Ltd.) was dissolved into 5 ml of water with 2.5 ml of formaline (guaranteed reagent, Kanto Chemical Co., Inc.). The solution obtained was added dropwise into 200 ml of 0.6 M KOH solution at 10 °C with stirring. The silver powder thus obtained was washed with water and dried in an oven at 120 °C.

Preparation of the Electrodes. The electrodes were prepared with the same method as in the previous work.[2] Poly(tetrafluoroethylene)(PTFE) (D-1, Daikin Industrial Company) was added to the catalyst powder in an amount proportional to 10% of the weight of the catalyst. The mixture was milled and dried to become a paste. The paste was calender-rolled by hand into sheets. They were used as catalyst layers.

The gas-side layers for the hydrogen-electrodes were prepared by binding nickel black powder with PTFE and by calender-rolling it into sheets.

Those for the oxygen-electrodes were prepared by using a mixture of graphite powder and activated carbon powder

---

† Present address: Fuji Electric Co., Ltd., Nagasaka, Yokosuka 240-01.

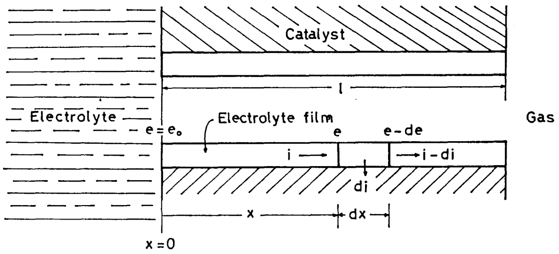

Fig. 1. Schematic cross section of an electrode pore.

instead of nickel black. After the sheets were reinforced with stainless steel screens (60—100 mesh), they were heated at 380 °C for 15 min in a nitrogen atmosphere. The gas-side layers thus obtained were attached to the catalyst layers by pressing at a pressure of 420 kg/cm^2. The double-layered electrodes obtained were heated in a hydrogen atmosphere at 150 °C for the hydrogen-electrodes and at 380 °C for the oxygen-electrodes.

Measurement of the Polarization. The geometrical working area of the electrodes was 7 cm^2. The electrolyte was a 6M KOH solution and was circulated at a rate of 5 ml/min. The electrolyte temperature was 60 ± 0.5 °C. The IR voltage drop was eliminated by the current-interruption method.$^{9)}$

Theoretical

When the PTFE-bonded electrodes contact with the electrolyte solution, the inner face of the electrode pore is covered with a thin electrolyte film while the electrolyte penetration into the central area of the pore is hindered by the repellency of PTFE. Thus the supplied gas can permeate the porous space to react with the electrolyte on the catalyst surface. This feature can be modeled as a cylindrical electrode pore as shown in Fig. 1. For the potential in the electrolyte film, e, Ohm's law holds:

$$\frac{de}{dx} + i\rho = 0, \tag{1}$$

where x is the distance from the electrode-face/electrolyte interface, i the ionic current density and ρ the resistivity of the electrolyte film. A linear function is assumed for the faradayic current density, di/dx:

$$\frac{di}{dx} + \frac{e}{k} = 0, \tag{2}$$

where k is the impedance for the inner-face/electrolyte interface per unit length of the pore. If ρ and k are independent of both x and e, and the edge effect of the pore can be neglected, Eqs. 1 and 2 can be integrated under the boundary conditions, $e=e_0$ at $x=0$ and $i=0$ at $x=l$:

$$e = e_0 \cdot \frac{\cosh\sqrt{\rho/k}(l-x)}{\cosh\sqrt{\rho/k}\,l} \tag{3}$$

$$i = \frac{e_0}{\sqrt{\rho k}} \cdot \frac{\sinh\sqrt{\rho/k}(l-x)}{\cosh\sqrt{\rho/k}\,l}, \tag{4}$$

where l is the length of the pore. Substituting $x=0$ into Eq. 4 one can obtain a potential-current relation to compare with experimental data:

$$i = \frac{e_0}{\sqrt{\rho k}} \cdot \tanh\sqrt{\rho/k}\,l. \tag{5}$$

Regarding e_0 as the polarization corrected for IR voltage drop, i as the current density per unit working area of the electrode, l as the thickness of the catalyst layer, ρ as the resistivity of the electrolyte film per unit working area of the electrode whose catalyst layer has unit thickness, and k as the impedance per unit thickness of the catalyst layer, one can apply Eq. 5 to the calculation of the polarization curves. The polarization resistance, ω, is defined as

$$\omega \equiv \left(\frac{e}{i}\right)_{x=0} = \sqrt{\rho k}\coth\sqrt{\rho/k}\,l. \tag{6}$$

The polarization resistance is the slope of the polarization curves and its application is limited to linear polarization characteristics. For application to the curves, they are divided into several segments with polarization values at intervals of 10—20 mV and Eq. 6 is then applied to each segment, regarding it as a straight line. From the polarization curves observed for various catalyst loadings, the reciprocal polarization resistance ω^{-1} can be calculated as a function of the thickness of the catalyst layer l for each of the polarization regions. Thus ρ and k are obtained as values that make curves for Eq. 6 best fit the observed ω^{-1} *vs.* l plots.

The faradayic current density, i_F, can be obtained as a function of x by substituting Eq. 3 into Eq. 2:

$$i_F \equiv \left|\frac{di}{dx}\right| = \frac{e_0}{k} \cdot \frac{\cosh\sqrt{\rho/k}(l-x)}{\cosh\sqrt{\rho/k}\,l}. \tag{7}$$

The ratio of i_F at $x=x$ to that at $x=0$, i_F/i_F°, is given by

$$\frac{i_F}{i_F^\circ} = \frac{\cosh\sqrt{\rho/k}(l-x)}{\cosh\sqrt{\rho/k}\,l}. \tag{8}$$

The above equation gives the profile of the faradayic current density across the electrode wall.

Results

Figure 2 shows plots of the polarization, η, against current density, I, measured for Raney nickel hydrogen-electrodes with variation of the catalyst loading. The ω^{-1} *vs.* l plots obtained from the data above are represented in Fig. 3, where the catalyst loading is given as the scale of the thickness of the catalyst layer; the conversion factor was obtained by measuring the thickness of the catalyst layers with a micrometer as 0.01 cm thickness=30 mg/cm^2 loading. The solid lines in the figure are the calculated curves of the best fit. The ρ and k values yielding the best fitting curves are shown in Table 1. The solid lines in Fig. 2 are polarization curves calculated from these parameter values using Eq. 5. The agreement with the observed plots is good.

As seen in Fig. 3, the ω^{-1} values reaches 90% of their upper limits when $l=4\times10^{-2}$ cm. Hence one centimeter was used as an l value that gives the upper limit of ω^{-1}. Line 1 in Fig. 2 is a polarization curve calculated for $l=1$ cm holding ρ and k to the values in Table 1. This is the best performance that can be theoretically expected using the Raney nickel catalyst prepared in the present study. If the catalytic activity is improved to yield $k=1.7\times10^{-3}$ Ω cm^3, which

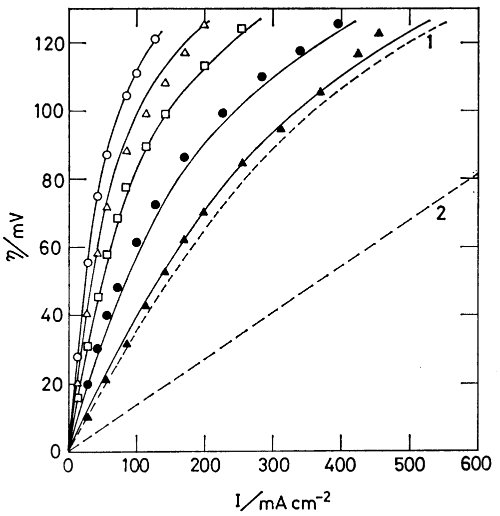

Fig. 2. Polarization curves for PTFE-bonded Raney nickel hydrogen-electrodes, IR drop eliminated. Electrolyte: 6 M KOH, 60 °C. Catalyst loading: ○; 15.15 mg/cm^2, △; 21.06 mg/cm^2, □; 31.74 mg/cm^2, ●; 61.6 mg/cm^2, ▲; 130.8 mg/cm^2. Solid line: Calculated using parameter values for the best fit, Line 1: Calculated for observed ρ and k values and $l=1$ cm, Line 2: Calculated for $k=1.7\times10^{-3}\ \Omega\ \mathrm{cm}^3$, $\rho=11\ \Omega$ cm and $l=1$ cm.

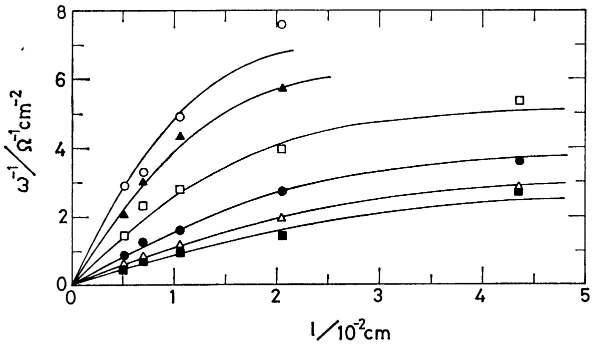

Fig. 3. Reciprocal polarization resistance as a function of thickness of the catalyst layer for PTFE-bonded Raney nickel hydrogen-electrodes.
Polarization region: ■; 0—40 mV, △; 40—60 mV, ●; 60—80 mV, □; 80—100 mV, ▲; 100—110 mV, ○; 110—120 mV. Solid lines: Calculated for the best fit.

is the value for the polarization of 110—120 mV, the polarization curve to be expected is given by Line 2 in the same figure.

Figure 4 shows polarization curves observed for the silver oxygen-electrodes. The ω^{-1} *vs.* l plots are shown in Fig. 5 where the conversion factor 0.01 cm thickness=40 mg/cm^2 loading (obtained by the thickness measurement) was used for the conversion of the loading to the thickness. The parameter values for the best fit are given in Table 2. The polarization curves calculated from these ρ and k values are shown by solid lines in Fig. 4. The agreement with the observed data is good except in highly polarized regions. The best performance attainable by the silver catalyst prepared in the present study is shown with Curve 1 in Fig. 6 which was calculated for the values

Table 1. The k values for the best fit in the PTFE-bonded Raney nickel hydrogen-electrodes[a)]

η / mV	k / $\Omega\ \mathrm{cm}^3$
0—40	1.1×10^{-2}
40—60	8.7×10^{-3}
60—80	6.0×10^{-3}
80—100	3.5×10^{-3}
100—110	2.2×10^{-3}
110—120	1.7×10^{-3}

a) A constant value of 11 Ω cm was used as a ρ value.

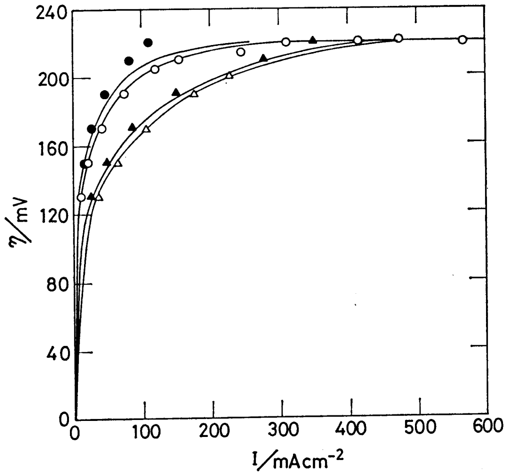

Fig. 4. Polarization curves for PTFE-bonded silver oxygen-electrodes, IR drop eliminated.
Electrolyte: 6 M KOH, 60 °C. Catalyst loading: ●; 22.5 mg/cm^2, ○; 28 mg/cm^2, ▲; 109 mg/cm^2, △; 127 mg/cm^2. Solid lines: Calculated using parameter values for the best fit.

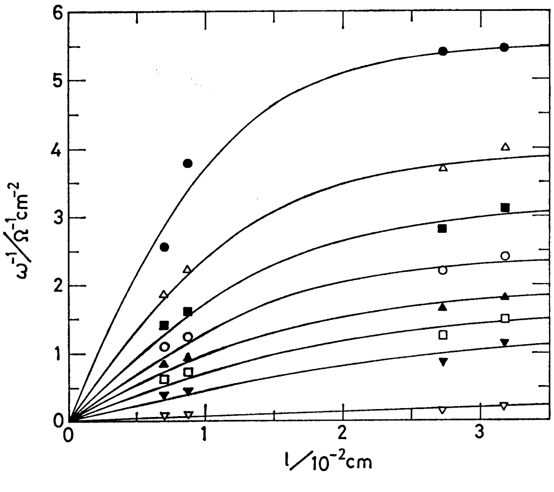

Fig. 5. Reciprocal polarization resistance as a function of thickness of the catalyst layer for PTFE-bonded silver oxygen-electrodes.
Polarization region: ▽; 0—120 mV, ▼; 120—140 mV, □; 140—150 mV, ▲; 150—160 mV, ○; 160—170 mV, ■; 170—180 mV, △; 180—190 mV, ●; 190—200 mV. Solid lines: Calculated for the best fit.

Table 2. The ρ and k values for the best fit in the PTFE-bonded silver oxygen-electrodes

$\frac{\eta}{\text{mV}}$	$\frac{\rho}{\Omega\ \text{cm}^3}$	$\frac{k}{\Omega\ \text{cm}^3}$
0—120	150	1.0×10^{-1}
120—140	30	2.0×10^{-2}
140—150	30	1.3×10^{-2}
150—160	30	9.2×10^{-3}
160—170	25	6.8×10^{-3}
170—180	20	5.1×10^{-3}
180—190	18	3.6×10^{-3}
190—200	15	2.2×10^{-3}
200—210	15	1.2×10^{-3}
210—215	15	5.4×10^{-4}
215—219	15	2.2×10^{-4}
219—220	15	8.0×10^{-5}

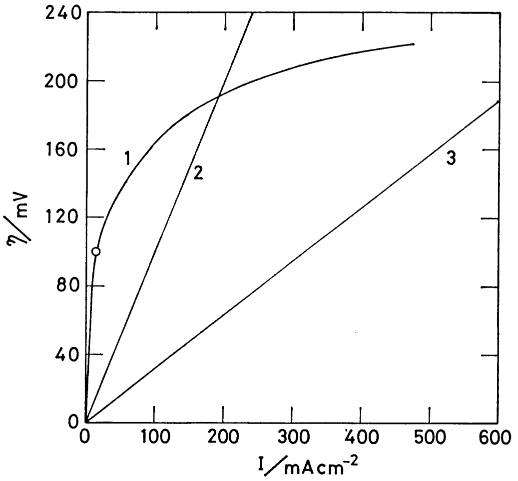

Fig. 6. Calculated polarization curves for silver oxygen-electrodes.
Line 1: Calculated for observed ρ and k values and $l=1$ cm observed datum for $l=0.0318$ cm, Line 2: Calculated for $k=0.1\ \Omega\ \text{cm}^3$, $\rho=10\ \Omega$ cm and $l=1$ cm, Line 3: Calculated for $k=0.01\ \Omega\ \text{cm}^3$, $\rho=10\ \Omega$ cm and $l=1$ cm.

of Table 2 and $l=1$ cm. It is very close to the open triangles in Fig. 4 (data for the thickest catalyst layer used in this study). Thus no marked improvement in the performance can be expected from thicker electrodes when the same catalyst is used. If the ρ value can be lowered to $10\ \Omega$ cm and $k=0.1\ \Omega$ cm³, Line 2 can be expected as the best performance. If the k value is lowered to $10^{-2}\ \Omega\ \text{cm}^3$ in addition to the above lowering in the ρ value, the best performance attainable is given by Line 3.

Discussion

When the polarization curves are divided into segments, there is a choice of sectionalizing with respect either to polarization or current density. When polarization was chosen, it was assumed implicitly that ρ and k depend upon polarization rather than current density. This assumption was open, but the good agreement found between the calculated and observed plots suggests the validity of the assumption employed.

As seen in Tables 1 and 2, the k values of both the hydrogen- and oxygen-electrodes decrease with progression of the polarization. This is due to an enhancement of the catalytic activity which is probably brought about by polarizing the electrode catalyst. As the hydrogen-electrode is polarized to a noble potential as a result of loading current, the Raney nickel catalyst is apt to accept oxygen onto the surface so that the concentration of the oxygen atom on the surface increases.

It has been recently suggested that the precipitates of oxides or hydroxides dispersed on the metal catalysts not only prevent the catalysts from diminishing the reactive area, but also accelerate the catalytic reaction through unknown metal-oxide interactions.10–15) Also, in the Raney nickel studied, a slight oxidation of the surface that does not reach the formation of non-conductive oxide film may enhance the catalytic activity for the electrode reaction. Attributing these polarization-induced activating effect for the Raney nickel catalyst to the activating effect of the oxide precipitates, we may identify the decrease in the k values due to polarization with the slightly oxidized surface state as described above. The plots deviate upward from the calculated curves in highly polarized regions, suggesting however that too much oxidation is harmful to the catalytic action.

The silver catalyst is also activated with progression of the polarization (Table 2). Contrary to the case of the hydrogen electrodes, this may be ascribed to surface reduction since the decrease in the k value results from polarizing to a less noble potential. No signs of loss of catalytic activity are observed in the region of high polarization.

In the silver oxygen-electrode studied, a total polarization required to sustain a load of 600 mA/cm² is 220 mV, but more than 120 mV out of the total value is expended for an initial 10 mA/cm² load. To improve the performance of this electrode, therefore, the reduction of the polarization, particularly in the low load current, is necessary. As expected from Eq. 5, the upper limit of ω^{-1} decreases with increasing ρ for a given k value. The ρ value of the oxygen-electrode studied is as high as $150\ \Omega$ cm in the polarization region 0—120 mV (Table 2). This very large value limits ω^{-1} to a very low value and results in only a poor electrode performance. Hence an enhancement in the conductivity of the electrolyte film is needed to improve the polarization characteristics.

Höhne has prepared oxygen-electrodes catalyzed with silver powder coprecipitated with metal hydroxides.16) His electrode is less polarized than the electrode prepared in the present study: The polarization of his electrode is 60 mV at a load of 40 mA/cm² while that of the present electrode is 130 mV at the same load. The same analytical method was applied to his polarization data to estimate the ρ and k values with assuming the same weight of the catalyst layer per 1 cm³. The parameter values obtained by the analysis are $\rho=15\ \Omega$ cm and $k=4.3\times10^{-3}\ \Omega\ \text{cm}^3$ in a low load current. These are smaller than the values ob-

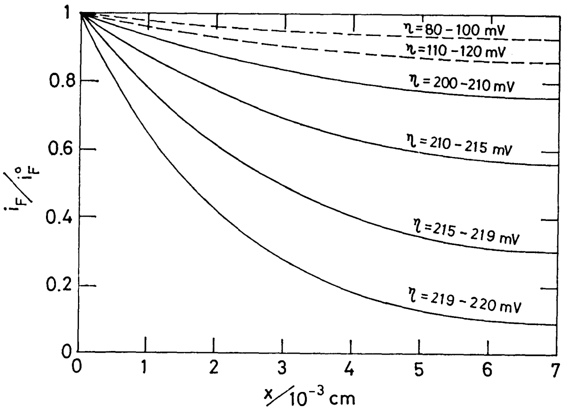

Fig. 7. Profiles of the faradayic current density across the electrode face.
Solid lines: Silver oxygen-electrodes, broken lines: Raney nickel hydrogen-electrodes, $l=7\times10^{-3}$ cm and the ρ and k values in Table 2 used for the calculation.

tained in the present study for the same load current. Höhne's electrodes were dried at 100 °C and no further heat treatment was applied, while the present electrodes were heated at 380 °C to remove the surfactant which had been originally introduced in the PTFE dispersion. The heat treatment at high temperatures deprives the catalyst of wettability and the reactive surface areas. In addition, the co-precipitated hydroxides may enhance the reactive surface area and the wettability of the catalyst. These two factors lower both the ρ and k values, but the lowering in the ρ value is the more important reason for bringing about the better performance.

The profiles for the faradayic current density across the electrode face were calculated for the parameter values in Tables 1 and 2 using Eq. 8. The results are given in Fig. 7. In contrast to the almost flat profiles for the hydrogen electrodes, the current densities for the silver electrodes are localized to the electrode-face/electrolyte interface as the electrodes are polarized; at $\eta=220$ mV, such a thin area of 5.3×10^{-3} cm thickness sustains 90% of the total load. If electrodes thicker than the above value are employed, the portion of the catalyst layer exceeding this thickness makes hardly any contribution to the improvement of the performance. Since the electrode preparation has usually been performed in the thicker region than the above value, the performance of the silver electrodes appears to be less dependent upon the catalyst loading than that of the Raney nickel electrodes. If thinner electrodes can be prepared and their polarizations measured, the dependence of the catalyst loading will be obtained more effectively.

This marked current localization is ascribed to the small k values of silver catalyst (Table 2), as is expected from Eq. 8. The large k values for Raney nickel catalyst, on the other hand, yield almost flat profiles, leading to long-ranging reaction zones. Thus the performance continues to enhance over the long distance in the coordinate of the electrode thickness (Fig. 3). Consequently, in the case of Raney nickel catalyst, thick electrodes yield good performance.

References

1) K. Mund, G. Richter, and F. von Sturm, *J. Electrochem. Soc.*, **124**, 1 (1977).

2) T. Kenjo, *Bull. Chem. Soc. Jpn.*, **54**, 2553 (1981).

3) N. Nakajima, Thesis, Muroran Institute of Technology, Muroran, 1981.

4) K. Koseki, T. Ihara, H. Tajima, and T. Kobayashi, The 22nd Battery Symposium in Japan, Kyoto, November 1981, Abstr. No. A19.

5) K. Mund, *Siemens Forsch.-u. Entwickel.-Ber.*, **4**, 1 (1975).

6) K. Mund, *Siemens Forsch.-u. Entwickel.-Ber.*, **4**, 68 (1975).

7) S. Srinivasan, H. D. Hurwitz, and J. O'M. Bockris, *J. Chem. Phys.*, **46**, 3108 (1967).

8) K. Micka, "Fuel Cell Systems," American Chemical Society, Washington, D. C. (1965), p. 73.

9) K. V. Kordesch and A. Marko, *J. Electrochem. Soc.*, **107**, 480 (1960).

10) F. von Sturm, "Proceeding of the Symposium on Electrode Materials and Processes for Energy Conversion and Storage," ed by J. D. E. Mclntyre, S. Srinivasan, and F. G. Will, The Electrochemical Society, Princeton, New Jersey (1977), pp. 247—264.

11) K. Kinoshita, "Proceedings of the Workshop on the Electrocatalyst of Fuel Cell Reactions," ed by W. E. O'Grady, S. Srinivasan, and R. F. Dudley, The Electrochemical Society, Princeton, New Jersey (1979), pp. 144—164.

12) A. Katayama, *Chem. Lett.*, **1978**, 1263.

13) M. Nakamura, 47th National Meeting of the Electrochemical Society of Japan, Yokohama, April 1980, Abstr. No. C 204.

14) S. J. Tauster, S. C. Fung, and R. L. Garten, *J. Am. Chem. Soc.*, **100**, 170 (1978).

15) R. T. Baker, E. B. Prestridge, and R. L. Garten, *J. Catal.*, **56**, 390 (1979).

16) K. Höhne, *Siemens Forsch-u. Entwickel.-Ber.*, **3**, 31 (1974).